The 3D multi-layered solvable six-vertex model: The phase diagram

1997 J. Phys. A: Math. Gen. 30 99

(http://iopscience.iop.org/0305-4470/30/1/008)

J. Phys. A: Math. Gen. **30** (1997) 99–116. Printed in the UK PII: S0305-4470(97)75687-7

The 3D multi-layered solvable six-vertex model: The phase diagram

V Popkov†§ and B Nienhuis‡

† Center for Theoretical Physics, Seoul National University, Seoul 151-742, Korea

‡ Institute for Theoretical Physics, University of Amsterdam, Valckernierstraat 65, NL 1018 XE, Amsterdam, the Netherlands

Received 14 July 1996, in final form 18 September 1996

Abstract. An anisotropic statistical model on a cubic lattice consisting of locally interacting six-vertex planes solvable via Bethe ansatz (BA), is studied. Symmetries of BA lead to an infinite hierarchy of possible phases, which is further restricted by numerical simulations. The model is solved for an arbitrary value of the interlayer coupling constant. Resulting is the phase diagram in general three-parameter space. Two new phases of chiral (spiral) character and a new first-order phase transition appear due to the interplane interaction. Exact mapping onto the models with some inhomogeneous sets of interlayer coupling constants is established.

1. Introduction

Exactly solvable models, e.g. models for which set of physical quantities such as the bulk free energy, the interfacial tension, some critical exponents, etc, can be calculated analytically, play an important role in statistical mechanics and the phase transitions theory. Most solvable statistical models are two-dimensional (see [1] for review). The Yang–Baxter equation, or the star–triangle equation, serves as an integrability condition, or a transfer-matrices commutativity condition for 2D solvable models. Unlike 2D models, solvable models in 3D are very rare examples. Usually solvable 3D models—see e.g. the Zamolodchikov model [2] and its generalizations [3]—are based on a solution of the tetrahedron equation. The latter is a natural generalization of the Yang–Baxter equation, YBE, and serves as transfer-matrices in the 3D commutativity condition.

Unfortunately all 3D solvable models known so far possess a common rather unsatisfactory feature, from the viewpoint of applications to statistical mechanics—they incurably have negative [2] or even complex [3] Boltzmann weights. Since these weights are probabilities (up to a normalization), this property makes the statistical mechanical interpretation of the models highly problematical (although the associated quantum problem may still be sensible).

Recently a method was proposed in [5, 6] which allows one to construct solvable statistical models (however, anisotropic) with positive Boltzmann weights and local interactions in 3D starting from solvable 2D models. The idea is the following. The whole row of an infinite number of separate sites (vertices) is considered as a simplest object. The state probabilities (Boltzmann weights) are defined as the product of those for each site separately, multiplied by the interaction factors depending upon the local configurations

§ On leave from: Institute for Low Temperature Physics, 47 Lenin Avenue, 310164 Kharkov, Ukraine.

0305-4470/97/010099+18$19.50

of each of the two neighbouring sites. Such construction leads to multilayered models on a 3D lattice, consisting of 2D integrable plane-layers, with specific interaction between them. What is important is that transfer-matrix commutativity condition turns out not to be a tetrahedron equation, but an infinite set of usual Yang-Baxter equations. These equations can be satisfied simultaneously, producing the variety of 3D-extended models [6] satisfying the necessary physical requirements—positivity of Boltzmann weights and locality of interactions.

Here we investigate the simplest example of such a model—the 3D-extended six-vertex model, with a homogeneous set of interplane coupling constants. The six-vertex model is a rather popular subject to study, as it is the limiting case for many solvable models in the critical region (see e.g. [1]). The 3D solvable extension for the six-vertex model was obtained in [5], and in [6] generalized to other solvable vertex models with charge conservation and inhomogeneous sequences of interplane interaction constants. In [5] the phase diagram for the free-fermion case was conjectured. Here we go beyond this restriction and obtain the phase diagram in the general three-parameter space, for the extended six-vertex model.

The paper is organized as follows. First we recall the definition of the anisotropic 3D-extended six-vertex model and consider the strong interplane interaction limit. Then we give the alternative derivation of the Bethe ansatz (BA) equations, using the established gauge equivalence of our multilayer model to the set of 2D six-vertex planes, each one in a field defined by the polarization of planes (neighbours). Using the symmetries of BA, we prove the equivalence between the model with a homogeneous set of interaction constants and some models with inhomogeneous sets. We make use of these results, together with hypothesis of non-degeneracy of maximal eigenvalue, to eliminate the problem. The resulting phase diagram is obtained in the next section. A conclusion and a discussion of the possible generalizations ends the paper.

2. Definition of the model

The model we consider is a system of K planes. Each of these planes is the symmetric six-vertex solvable model on a square $N \times M$ lattice [8]. We can 'paste' together ij-sites of all planes and formally get a 2D system with a complex site consisting of K simple vertices (see figure 1).

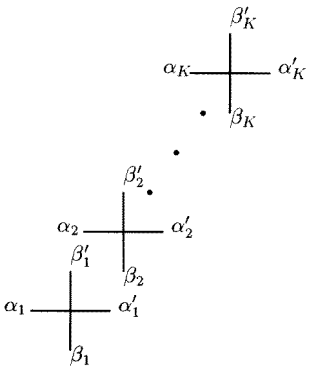

Figure 1. Multivertex consisting of K simple vertices.

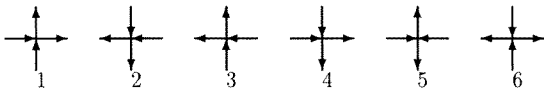

Figure 2. Permissible vertex configurations for the six-vertex model. Boltzmann weights of configurations $w_1 = w_2 = a$; $w_3 = w_4 = b$; $w_5 = w_6 = c$.

The Boltzmann weight of such a multivertex fragment has the form

$$\mathsf{L}^{\alpha_1\alpha_2\ldots\alpha_K\beta_1\beta_2\ldots\beta_K}_{\alpha'_1\alpha'_2\ldots\alpha'_K\beta'_1\beta'_2\ldots\beta'_K} = \prod_{k=1}^{K} L_{6v}{}^{\alpha_k,\beta_k}_{\alpha'_k,\beta'_k} \exp\{-h_k\alpha_k\beta_{k+1} + h_k\alpha'_{k+1}\beta'_k\} \tag{1}$$

where h_k are arbitrary constants, defining the interaction between nearest neighbours in the kth and $(k+1)$th plane, $L_{6v}{}^{\alpha_k,\beta_k}_{\alpha'_k,\beta'_k}$—the Boltzmann weights of the 'source' six-vertex solvable model [9], state variables $\alpha_k, \beta_k, \ldots$ take values ± 1. For the planes (layers) we impose periodic boundary conditions $K + 1 \equiv 1$. The permissible configurations of the six-vertex model are drawn on figure 2. The variables sitting on edges are represented by arrows in figure 2. '+' ('−') correspond to arrows pointing up or to the right (down or to the left). The local Boltzmann weights are invariant under inversion of all arrows.

2.1. Strong interplane interaction limit $h \to \infty$

To understand the nature of the interaction for the homogeneous model (all interplane interaction constants h_k equal: $h_k \equiv h$, any k), let us consider the strong interplane interaction limit $h \to \infty$. The configuration with maximal Bolzmann weight will give the main contribution to the partition sum. To obtain this configuration, we should maximize the exponential factor in (1) for all sites in all planes.

Without loss of generality, we can set $\alpha_k = \beta'_k = +1$ for the kth plane. Then, to maximize the exponential factor in (1), we should choose $\beta_{k+1} = -1$; $\alpha'_{k+1} = +1$ in the $(k+1)$th plane, i.e. vertex of type 4 (see figure 2), and $\alpha_{k+1} = +1$; $\beta'_{k+1} = -1$. Performing the next step, we get $\beta_{k+2} = \alpha'_{k+1} = -1$. This fits vertices of type 5 and 2; however, vertex 5 is unsuitable†. Proceeding analogously further, we get: planes k–$(k+4)$ are formed by the vertices of type 1, 4, 2, 3 and 1, respectively. It is easy to see that each vertex (each plane) can be obtained from the previous one by a clockwise rotation of $\pi/2$. After full rotation over 2π, the configuration repeats.

Thus, in the strong interplane interaction limit, the model has a homogeneous structure within each horizontal plane, and a spiral structure with period 4 in the vertical direction: each plane configuration is obtained from the previous one by a clockwise $\pi/2$ rotation:

$$\ldots \nearrow \searrow \swarrow \nwarrow \ldots. \tag{2}$$

The arrows in the formula above result from a vector summation of all arrows in each plane: for example, the arrow $\nearrow$ corresponds to a homogeneous configuration of vertices of type 1 in figure 2.

† In order to get the maximal Boltzmann weight, we have to construct a configuration in each plane with the same types of vertices. This can be done with type 1–4 vertices but not with type 5 vertices—they always go in pairs with type 6 vertices.

3. The matrix formulation

It is convenient to rewrite (1) in matrix form. Let us introduce the $2^{2K} \times 2^{2K}$ matrix $\mathcal{L}^k$ acting in the tensor product $\prod_1^K \otimes g_0 \prod_1^K \otimes g_n$ with elements

$$(\mathcal{L}^k)^{\alpha_1\alpha_2\ldots\alpha_K\beta_1\beta_2\ldots\beta_K}_{\alpha'_1\alpha'_2\ldots\alpha'_K\beta'_1\beta'_2\ldots\beta'_K} = \delta_{\alpha_1\alpha'_1}\delta_{\beta_1\beta'_1}\delta_{\alpha_2\alpha'_2}\delta_{\beta_2\beta'_2}\ldots\delta_{\alpha_{k-1}\alpha'_{k-1}}\delta_{\beta_{k-1}\beta'_{k-1}} \times \exp(-h_k\alpha_k\beta_{k+1} + h_{k-1}\alpha'_k\beta'_{k-1}) L_{6v}{}^{\alpha_k\beta_k}_{\alpha'_k\beta'_k}\delta_{\alpha_{k+1}\alpha'_{k+1}}\delta_{\beta_{k+1}\beta'_{k+1}}\ldots\delta_{\alpha_K\alpha'_K}\delta_{\beta_K\beta'_K}. \tag{3}$$

L_{6v} is the 4×4 local L-matrix of the six-vertex model with the following nonzero elements:

$$L^{11}_{11} = L^{22}_{22} = a \qquad L^{12}_{12} = L^{21}_{21} = b \qquad L^{12}_{21} = L^{21}_{12} = c \tag{4}$$

in which a, b, c are Boltzmann weights of permissible configurations (see figure 2). Here and below in this section we borrow notations from the paper of Takhtajan and Faddeev [4]. Note that matrices $\mathcal{L}^k$, corresponding to neighbouring ks, do not commute. The multivertex Boltzmann weights (1) are matrix elements of the ordered matrix product of $\mathcal{L}^k$ over all planes:

$$\prod_{k=1}^{K}\mathcal{L}^k = \mathbf{L}$$
$$\mathbf{L}^{\alpha_1\alpha_2\ldots\alpha_K\beta_1\beta_2\ldots\beta_K}_{\alpha'_1\alpha'_2\ldots\alpha'_K\beta'_1\beta'_2\ldots\beta'_K} = \prod_{k=1}^{K} L_{6v}{}^{\alpha_k,\beta_k}_{\alpha'_k,\beta'_k}\exp\{-h_k\alpha_k\beta_{k+1} + h_{k-1}\alpha'_k\beta'_{k-1}\} \tag{5}$$

(expressions (1) and (5) are the same, due to periodicity).

Using the notations introduced we can write the partition function of the model in the usual (see e.g. [1]) form:

$$\mathbf{Z} = \mathrm{Tr}(\mathbf{T})^M \tag{6}$$

with transfer-matrix $\mathbf{T}$ being the trace of the ordered product of local matrices $\mathbf{L}$ along the row (we shall denote matrix $\mathbf{L}$ acting in the site n as $\mathbf{L}_n$):

$$\mathbf{T} = \mathrm{Tr}\left(\prod_{n=1}^{N}\mathbf{L}_n\right). \tag{7}$$

Here the Tr operation and the matrix product go over α-indexes (we shall call it the 'auxiliary' space) and the Tr operation in the previous formula (6) goes over β-indexes ('quantum' space).

The free energy per site in the thermodynamic limit $N, M, K \to \infty$ is defined by the maximal transfer-matrix eigenvalue

$$\mathbf{T}\Psi = \mathbf{\Lambda}\Psi \qquad f = -k_\mathrm{B}T\lim_{N,K\to\infty}\frac{1}{NK}|\mathbf{\Lambda}_{max}|. \tag{8}$$

An important feature of our K-plane model is that its monodromy matrix $\mathcal{T}$ can be written as an ordered product of more simple ones (we shall denote matrix $\mathcal{L}^k$ from (3) acting in the site n as $\mathcal{L}^k_n$):

$$\mathcal{T} = \prod_{n=1}^{N}\mathbf{L}_n = \prod_{n=1}^{N}\left(\prod_{k=1}^{K}\mathcal{L}^k_n\right) = \prod_{k=1}^{K}\left(\prod_{n=1}^{N}\mathcal{L}^k_n\right) = \prod_{k=1}^{K}\mathcal{T}_k \tag{9}$$

$$\mathcal{T}_k = \prod_{n=1}^{N}\mathcal{L}^k_n. \tag{10}$$

Matrix $\mathcal{L}^k$ from (3) can be written in a compact form as can be easily verified:

$$\mathcal{L}^k = \exp(-h_k \sigma^{(k)} \tau^{(k+1)}) L_{6v}{}^k \exp(h_{k-1} \sigma^{(k)} \tau^{(k-1)}) \tag{11}$$

where we denote by the $\sigma^{(k)}$ and $\tau^{(k)}$ the diagonal matrix $\sigma^z = \mathrm{diag}(1, -1)$ acting nontrivially in the kth 'auxiliary' and the kth 'quantum' space, respectively:

$$\begin{aligned}
(\sigma^{(k)})^{\alpha_1\alpha_2\ldots\alpha_K\beta_1\beta_2\ldots\beta_K}_{\alpha'_1\alpha'_2\ldots\alpha'_K\beta'_1\beta'_2\ldots\beta'_K} &= \delta_{\alpha_1\alpha'_1}\ldots\delta_{\alpha_{k-1}\alpha'_{k-1}}(\sigma^z)_{\alpha_k\alpha'_k}\delta_{\alpha_{k+1}\alpha'_{k+1}}\ldots\delta_{\alpha_K\alpha'_K}\prod_{i=1}^{K}\delta_{\beta_i\beta'_i} \\
(\tau^{(k)})^{\alpha_1\alpha_2\ldots\alpha_K\beta_1\beta_2\ldots\beta_K}_{\alpha'_1\alpha'_2\ldots\alpha'_K\beta'_1\beta'_2\ldots\beta'_K} &= \delta_{\beta_1\beta'_1}\ldots\delta_{\beta_{k-1}\beta'_{k-1}}(\sigma^z)_{\beta_k\beta'_k}\delta_{\beta_{k+1}\beta'_{k+1}}\ldots\delta_{\beta_K\beta'_K}\prod_{i=1}^{K}\delta_{\alpha_i\alpha'_i}.
\end{aligned} \tag{12}$$

4. Bethe ansatz equations

It can be shown—see the appendix for a proof—that the 3D model under consideration (equation (1)) is gauge equivalent† to the set of 2D six-vertex planes, each in its own horizontal field with the strength defined by the vertical polarization in neighbouring planes and interplane interaction constants: for the kth plane the field strength

$$H_k = h_k y_{k+1} - h_{k-1} y_{k-1} \tag{13}$$

where polarization y_k is defined as usual:

$$y_k = \frac{n_k^{\uparrow} - n_k^{\downarrow}}{n_k^{\uparrow} + n_k^{\downarrow}} = \frac{2n_k^{\uparrow} - N}{N}. \tag{14}$$

$n_k^{\uparrow}$ ($n_k^{\downarrow}$) is the number of upward (downward) pointing arrows in a horizontal row in plane k.

Therefore, the Bethe ansatz of the model is given by the well known formulae for the six-vertex model in an external horizontal field (see e.g. [8]); below, $n_k = n_k^{\uparrow}$, $y_k = \frac{2n_k - N}{N}$):

$$\Lambda_k(H_k) = a^N \mathrm{e}^{NH_k} \prod_{j=1}^{n_k} \frac{a\tau_j^{(k)} - b(2\Delta\tau_j^{(k)} - 1)}{a - b\tau_j^{(k)}} + b^N \mathrm{e}^{-NH_k} \prod_{j=1}^{n_k} \frac{b - a(2\Delta - \tau_j^{(k)})}{-a + b\tau_j^{(k)}} \tag{15}$$

where $\tau_j^{(k)}$ satisfy the set of Bethe ansatz equations

$$\begin{aligned}
&\mathrm{e}^{2NH_k}(\tau_j^{(k)})^N = (-1)^{n_k+1} \prod_{l=1}^{n_k} \frac{\tau_j^{(k)}\tau_l^{(k)} - 2\Delta\tau_j^{(k)} + 1}{\tau_j^{(k)}\tau_l^{(k)} - 2\Delta\tau_l^{(k)} + 1} \\
&n_k = 1, 2, \ldots N \qquad k = 1, 2 \ldots K
\end{aligned} \tag{16}$$

where

$$\Delta = \frac{a^2 + b^2 - c^2}{2ab} \tag{17}$$

a, b, c are Boltzmann weights of a symmetrical six-vertex model configurations (see figure 2).

The global transfer-matrix eigenvalue is the product of those over all planes:

$$\mathbf{\Lambda}^{\{h\}}_{\{y\}} = \mathbf{\Lambda}^{h_1,h_2\ldots h_K}_{y_1,y_2\ldots y_K} = \Lambda_{y_1}(H_1)\Lambda_{y_2}(H_2)\ldots\Lambda_{y_K}(H_K) \qquad y_p = \frac{2n_p - N}{N}. \tag{18}$$

† We thank Yury Stroganov for drawing our attention to this fact.

Equations (15), (16) were obtained directly in [5, 6] using the quantum inverse scattering method, and the analytic ansatz method, respectively.

We shall restrict ourselves to the model with all interplane interaction constants equal: $h_k \equiv h$, any k (below we refer to that case as the homogeneous model). However, as is shown below, our results are also valid for some models with inhomogeneous sequences $\{h_k\}$.

To obtain the bulk free energy and complete phase diagram, one should find a sequence of n_k, $\{n_k\}_{k=1}^{K}$ that corresponds to the maximal transfer-matrix eigenvalue Λ_{max}, and Λ_{max} itself, in complete three-parameter space $a/c,\ b/c,\ h$. This programme can be performed easily in the following limiting cases:

(1) For the single six-vertex model (decoupled planes limit $h = 0$). Then BA solutions $\tau_i^{(k)}$ lie on a unit circle $\tau_j^{(k)} = \mathrm{e}^{\mathrm{i}\lambda_j^{(k)}}$, $\lambda_j^{(k)}$ real. The expression for Λ_{max} is then found by the integral equation method (see e.g. [1]).

(2) The 'Ising chain' case $\Delta = \pm\infty$, i.e. $a = 0$ or $b = 0$, any h is equivalent to $\Delta = \pm\infty$, $h = 0$. Thus it is reduced to the previous case.

(3) For the free fermions case $\Delta = 0$. Then the RHS of (16) is equal to 1, and BA is solved trivially. The complete analysis is done in [5].

In the general case, i.e. nonzero h and Δ, the structure of BA equations does not permit simple analysis. The reason is that in that case the locus of BA roots is unknown. The problem is similar to that arising when one considers usual six-vertex model in external horisontal field (see [8, 1]).

4.1. Connections between models with interplane constants $\{\ldots h, h, h, h, \ldots\}$, $\{\ldots h, -h, h, -h, \ldots\}$, *and arbitrary sets of 'h' and '−h'*

The models listed in the title look different, and different they are, having, for instance, a different 'strong interplane interaction limit' $h \to \infty$ (this can be verified directly as was done for the homogeneous model at the beginning of the paper). We shall show, however, that they have precisely the same transfer-matrix spectrum, and therefore the same phase diagram, with minor redefinition of phases.

Let us take the state of the kth plane with n_k arrows pointing up, in a field H_k, described by equations (15), (16). Reversing all horizontal and vertical arrows, together with changing the sign of H_k, leaves the Boltzmann weights and therefore the eigenvalue (15) invariant:

$$\Lambda_{y_k}(H_k) = \Lambda_{-y_k}(-H_k) \tag{19}$$

(the Bethe ansatz (16) changes accordingly). Using this formula, we write the global transfer-matrix eigenvalue (18) for the set $\{y_1, y_2, -y_3, -y_4, y_5, y_6, -y_7, -y_8, \ldots - y_K\}$ for the homogeneous model:

$$\begin{aligned}\mathbf{\Lambda}^{h\ \ h\ \ h\ \ h}_{y_1\ y_2\ -y_3\ -y_4} &= \Lambda_{y_1}(h(y_2+y_K))\Lambda_{y_2}(h(-y_3-y_1))\Lambda_{-y_3}(h(-y_4-y_2))\Lambda_{-y_4}(h(y_5+y_3)) \\ &= \Lambda_{y_1}(h(y_2+y_K))\Lambda_{y_2}(h(-y_3-y_1))\Lambda_{y_3}(h(y_4+y_2))\Lambda_{y_4}(h(-y_5-y_3)).\end{aligned} \tag{20}$$

Remark. Here and below we assume the number of planes K to be infinitely large and divisible by all numbers $K = 2*3*4*\ldots$, $K+1 \equiv 1$, to avoid complications connected with the boundary effects. For the sake of simplicity we write down only the significant part of the multiplication (18), then it continues periodically.

Let us write down the global eigenvalue for the system with alternating constants:

$$\mathbf{\Lambda}^{h\ \ -h\ \ h\ \ -h}_{y_1\ y_2\ y_3\ y_4} = \Lambda_{y_1}(h(y_2+y_K))\Lambda_{y_2}(h(-y_3-y_1))\Lambda_{y_3}(h(y_4+y_2))\Lambda_{y_4}(h(-y_5-y_3)). \tag{21}$$

Comparing with the previous formula we have

$$\Lambda^{h\ \ h\ \ h\ \ h}_{y_1\ y_2\ -y_3\ -y_4} = \Lambda^{h\ \ -h\ \ h\ \ -h}_{y_1\ y_2\ y_3\ y_4} \tag{22}$$

(periodical continuation is implied—see remark above).

Analogously one obtains

$$\Lambda^{h\ \ h\ \ h\ \ h}_{y_1\ y_2\ y_3\ y_4} = \Lambda^{h\ \ h\ \ -h\ \ -h}_{y_1\ y_2\ y_3\ -y_4}. \tag{23}$$

Actually, one could coin such transformations between the model with homogeneous sequences and those with arbitrary sequences of 'h' and '$-h$': $\{h_k\}_{k=1}^K$, $h_k = \pm 1$, $k = 1, 2, \ldots K$. For instance,

$$\mathbf{\Lambda}^{h\ \ h\ \ -h}_{y_1\ y_2\ y_3} = \mathbf{\Lambda}^{h\ \ h\ \ h\ \ldots\ \ldots\ \ \ldots\ h}_{y_1\ y_2\ y_3\ -y_4\ -y_5\ -y_6} \tag{24}$$

and so on.

5. Symmetries

Here we make use of the results of the previous paragraph to establish transformations which map the eigenvalue to the eigenvalue of the same model.

First of all, note that simultaneous inversion of polarization in all planes Z

$$Z\{y\} = \{-y\} \tag{25}$$

leaves the eigenvalue invariant:

$$\mathbf{\Lambda}^{\{h\}}_{\{-y\}} = \prod_k \Lambda^{h_k}_{-y_k}(-h_k y_{k+1} + h_{k-1} y_{k-1}) = \prod_k \Lambda^{h_k}_{y_k}(h_k y_{k+1} - h_{k-1} y_{k-1}) = \mathbf{\Lambda}^{\{h\}}_{\{y\}}.$$

This is also the direct consequence of the fact that local Boltzmann weight (1) is invariant under the transformation *all* $\alpha_k, \beta_k \to -\alpha_k, -\beta_k$.

Another transformation we obtain, inverting the order of the $\{y\}$-set and the $\{-h\}$-set is as follows:

$$\mathbf{\Lambda}^{h_1, h_2 \ldots h_K}_{y_1, y_2 \ldots y_K} = \mathbf{\Lambda}^{-h_K\ \ -h_{K-1} \ldots\ldots -h_2 - h_1}_{y_1\ \ \ y_K\ \ y_{K-1} \ldots\ y_3\ \ y_2}$$

(this is proved analogously). Transformation J:

$$J\{y_1, y_2 \ldots y_K\} = \{y_1\ y_K\ \ y_{K-1} \ldots\ \ y_3\ \ y_2\} \tag{26}$$

is a symmetry for the model with alternating constants:

$$\mathbf{\Lambda}^{h\ -h\ h\ -h}_{\{y\}} = \mathbf{\Lambda}^{h\ -h\ h\ -h}_{J\{y\}}.$$

Then, one more independent symmetry exist for that model:

$$F\{y\} = \{y_2\ -y_3\ \ \ldots y_K\ -y_1\} \qquad \mathbf{\Lambda}^{h\ -h\ h\ -h}_{\{y\}} = \mathbf{\Lambda}^{h\ -h\ h\ -h}_{F\{y\}}. \tag{27}$$

For completeness, we define operator of the one-step shifting S:

$$S\{y\} = \{y_2\ y_3 \ldots\ y_K\ y_1\}. \tag{28}$$

Evidently, S^n, integer n, is a trivial symmetry for the homogeneous model and S^{2n} is a trivial symmetry for the model with alternating constants. Transformations Z, J, F, S^2 are basic symmetries for the model with alternating constants. Let us obtain the basic symmetries for the homogeneous case. Z and S are already symmetries.

Then, define the transformation from (22) between the two models:

$$Q\{y\} = \{y_1\ y_2\ -y_3\ -y_4 \ldots\} \qquad Q^{-1} = Q.$$

Transformations QJQ and QFQ are the symmetries sought for:

$$\begin{aligned} &P\{y\} = QJQ\{y\} = \{y_1\ -y_K\ y_{K-1}\ -y_{K-2}\dots y_3\ -y_2\} \qquad P^2 = I \\ &QFQ = S. \end{aligned} \tag{29}$$

So, for the homogeneous model *all* $h_k \equiv h$ two nontrivial symmetries Z and P exist defined by (25) and (29). Working out the same procedure for the model $h, h, -h, -h \dots$ does not give additional information. It is noteworthy also that the Z-symmetry is not independent but can be expressed in terms of shifting and P-symmetry

$$Z = (SP)^2.$$

Nevertheless it proves convenient to keep it in mind as a separate symmetry. As is shown below, Z and P symmetries, having been combined with the non-degeneracy hypothesis, put drastic constraints on the polarization set $\{y\}$ which corresponds to the maximal eigenvalue of the global transfer-matrix of the homogeneous model.

6. Finding the maximal eigenvalue set $\{y\}$

We are now in a position to solve the maximal eigenvalue problem, for the homogeneous model. First we have to point out which set $\{y\}$ corresponds to it for any value of parameters $a/c, b/c, h$. We shall parametrize the possible sets by a period T and define the set $\{y^{(T)}\}$ as that with periodically repeating entries:

$$\{y^{(T)}\} = \{y_1\ y_2 \dots\ y_T\ y_1\ y_2 \dots\ y_T \dots\ y_T\} \qquad \{y^{(T)}\}_{T+n} = \{y^{(T)}\}_n.$$

Note that cases $T = 1$ and $T = 2$ are trivial because they lead to vanishing of interaction h from all expressions (see (13)–(16)). The symmetry Z (see (25)) does not effect the period T of the set, but the symmetry (29) does. Having been applied for odd $T = 2n + 1$, it doubles the period:

$$P\{y^{(T)}\} = \{\tilde{y}^{(2T)}\}. \tag{30}$$

For instance for the period $T = 3$

$$P\{y_1\ y_2\ y_3\ \dots\} = \{y_1\ -y_3\ y_2\ -y_1\ y_3\ -y_2 \dots\}.$$

(We write down only the simplest periodically repeating pattern.)

Note that set $\{y^{(T)}\}$, odd T for the homogeneous model, corresponds to the sequence of period $4T$ for the model with alternating constants: $Q\{y^{(T)}\} = \{\tilde{y}^{(4T)}\}$.

For the sets with even $T = 2n$ the symmetry (29), generally speaking, does not effect the period, as can be easily verified.

To go further, we need an additional piece of information concerning the maximal eigenvalue set $\{y\}$. We supply it by stating:

The maximal eigenvalue set for the homogeneous model is unique, modulo shift, for all phases except the ferroelectric phase I (see figure 3).

This statement equates to stating that the maximal global transfer-matrix eigenvalue is non-degenerate. For the 'source' six-vertex model, this is true: $y = 0$ for all phases except ferroelectric, and $y = 0$ is just the value invariant under action of Z-symmetry (25). Strong coupling limit $h \to \infty$ is non-degenerate, too. As to the exclusion—ferroelectric phase I (see figure 3), it has degeneracy 2^K, K being the number of planes. Indeed the ferroelectric phase is built up from a- (or b-) vertices only. It follows from (1) that Boltzmann weight does not depend on h for the homogeneous model, whatever a-vertices (type 1 or type 2—see figure 2) form each plane.

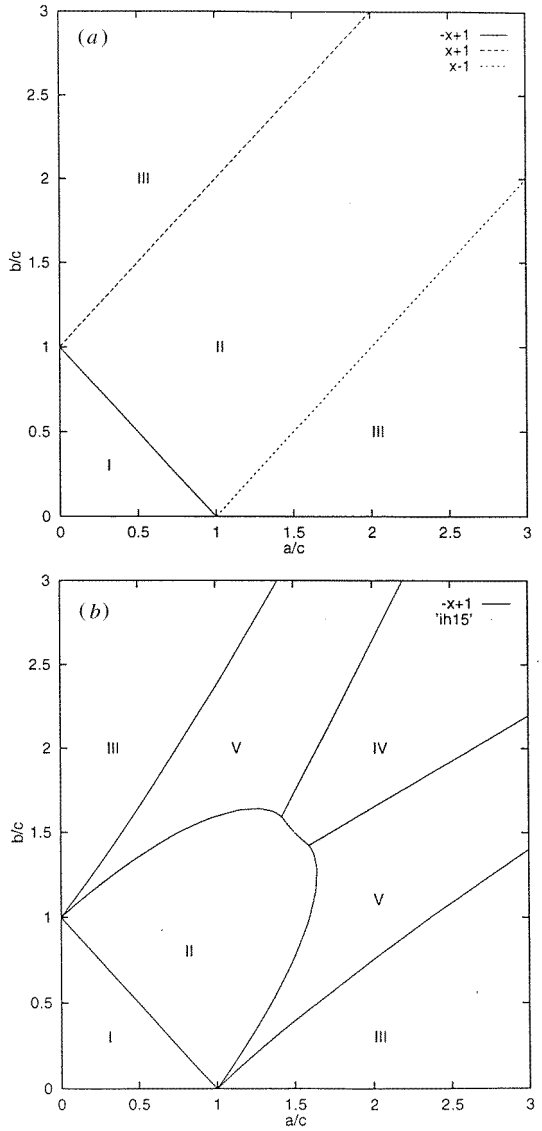

Figure 3. Phase diagrams of the 3D-extended six-vertex model on cubic lattice in the a/c, b/c plane, for the different values of interplane constant h. (a) decoupled planes limit $h = 0$; (b) $h = 0.15$; (c) $h = 0.3$; (d) $h = 0.5$. The phase transitions between the phases II/IV, II/V, V/III are of the first order. The phase transitions between the phases IV/V are of the second-order, Pokrovsky–Talapov-type. Transition I/II is the Kosterlitz–Thouless-type transition. Curves separating phases III/V, V/IV are given by: $\Delta = \cosh 4h$, $(b/c) = (a/c)\exp 4h - 1$, respectively.

For all other phases, the hypothesis of non-degeneracy means that the maximal set $\{y\}_{max}$ is invariant under action of Z- and P-symmetries (25), (29), modulo arbitrary shift†.

† Note that for the model with alternating constants $\{\ldots h,\ -h,\ h,\ -h, \ldots\}$, the maximal set $\{y\}_{max}$ is always degenerate. It is the additional symmetry F (27) that accounts for the degeneracy. The same holds for the model with the constants $\{\ldots h, h, -h, -h, \ldots\}$.

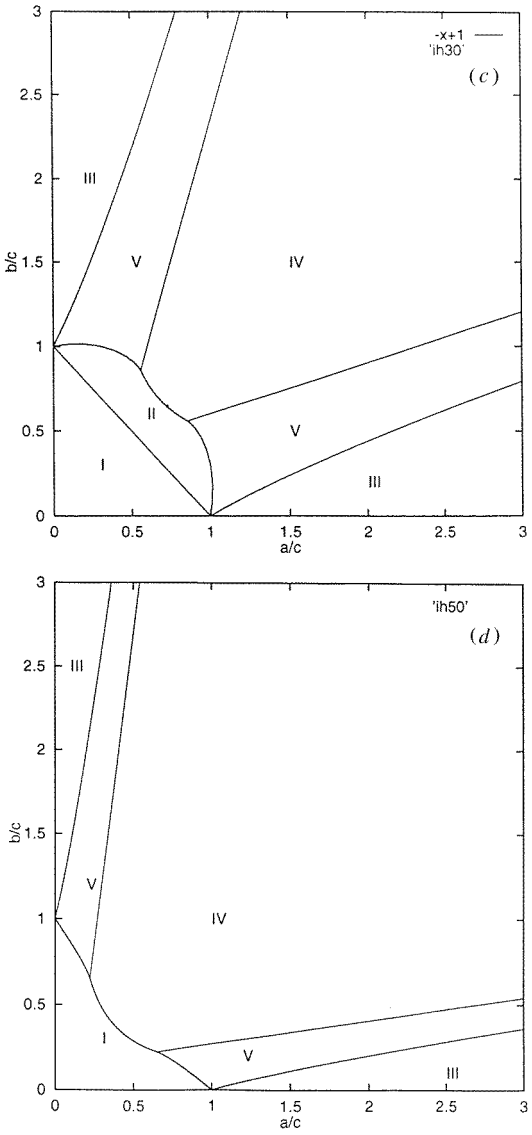

Figure 3. (Continued)

The immediate consequences are:

(1) From (25): that the average value of $\langle y_p \rangle_{max}$ must be zero:

$$\frac{1}{K}\sum_{p=1}^{K} y_p = 0.$$

(2) From (30): that the maximal set cannot have an odd period.

Also, the period of maximal set cannot be $T = 2n$, n odd. To see that, consider $T = 6$. For the set to be invariant under action of Z-symmetry (equation (25)) it must have form

$$\{y^{(6)}\} = \{u\ v\ w\ -u\ -v\ -w \ldots\}.$$

Acting on it by the P-symmetry

$$P\{y^{(6)}\} = \{u\ w\ -v\ldots\}$$

one obtains the set with period 3. Analogously one obtains $P\{y^{(2n)}\} = \{\tilde{y}^{(n)}\}$, n odd, in contradiction with the non-degeneracy hypothesis.

Since the maximal sets $\{y^{(T)}\}$ with T and $T/2$ odd are forbidden, we are left with the only possible choice

$$T = 4n.$$

For that case, $P\{y^{(4n)}\} = \{\tilde{y}^{(4n)}\}$ always.

The first nontrivial case is $T = 4$. Note that it is just the period which arises in the strong interplane interaction limit $h \to \infty$. According to Z-symmetry (or also to P-symmetry) invariance, the maximal set reads

$$\{y^{(4)}\} = \{\eta\ \xi\ -\eta\ -\xi\ldots\}. \tag{31}$$

6.0.1. $T = 8$. P- and Z-symmetry invariance lead to the following set:

$$\{y^{(8)}\} = \{u\ v\ 0\ v\ -u\ -v\ 0\ -v\ldots\}. \tag{32}$$

With increasing T, the admissible structure looks more and more complicated. For $T = 12$

$$\{y^{(12)}\} = \{u\ v\ w\ r\ -w\ v\ -u\ -v\ -w\ -r\ w\ -v\ldots\} \tag{33}$$

and so on. Thus, we have produced the hierarchy of sequences which are candidates for the planes polarization set $\{y\}_{max}$ corresponding to the maximal global transfer-matrix eigenvalue. The number of parameters is reduced essentially but still there is quite some freedom left. The results are in agreement with numerical data. The latter, however, forces us to formulate the final hypothesis which we cannot prove. It is described in the following section.

7. The final hierarchy

Let us assume that the maximal set contains at least one plane k with maximal polarization $y_k = 1$. It follows immediately from (25) and non-degeneracy, that some another plane p has $y_p = -1$. Denote the distance between these two planes by $A = |p - k|$. We shall parametrize the sequences $\{y\}$ by the value of A. The entries of maximal set $\{y\}_{max}$ obey the following rule:

$$\begin{aligned} y_{k+n} &= -y_{k-n} \qquad n \text{ odd} \\ y_{k+m} &= y_{k-m} \qquad m \text{ even} \end{aligned} \tag{34}$$

and the same with the replacement of k by any other number $\tilde{k}$, where $y_{\tilde{k}} = \pm 1$. From (34) those numbers are $\tilde{k} = k \pm An$, integer n. Making use of (34), for A odd we obtain the y-set of period $4A$ $\{y^{(4A)}\}$, and $\{y^{(2A)}\}$, for A even. The rules (34) are consistent with Z and P symmetries, and can be derived from them.

Let us take $A = 1$. Here we have

$$\{y\} = \{1\ 1\ -1\ -1\ldots\} \tag{35}$$

—just the maximal set for the $h \to \infty$ limit (phase 4 in the phase diagram). $A = 2$ produces the set

$$\{y\} = \{1\ -\xi\ -1\ \xi\ldots\} \tag{36}$$

—the maximal set for phase 5 in the phase diagram. It coincides with that from (32) when $\eta = 1$. For $A = 3$ one obtains from equations (34):

$$\{y\} = \{1\ v\ w\ -1\ -w\ v\ -1\ -v\ -w\ 1\ w\ -v \ldots\} \tag{37}$$

which coincides with (33) when $u = 1$, $r = -1$.

$A = 4$ produces the set (32) with the substitution $u = 1$, and so on.

Phases with $A = 1, 2$ do exist on the phase diagram. However, we have failed to find numerically the phases with $A = 3, 4$. From this we conclude that other members of hierarchy, with $A > 4$, do not appear, either. We suggest that the higher members of hierarchy do appear when one takes into consideration more distant than nearest neighbours' plane–plane interaction. For instance, we have checked that the phase with $A = 3$ (equation (37)) does enter the phase diagram when one includes additional interaction between the planes $k \to k + 3$, any k.

8. The phase diagram

We have shown in the last two sections that the set of polarization constants $\{y\} = y_1, y_2 \ldots y_K$ which corresponds to the maximal eigenvalue (the maximal set) must have the period divisible by 4: $T = 4n$. For the simplest case, $T = 4$, the maximal set is (31) and the transfer-matrix eigenvalue is given by equation (20), with the substitution $y_1 = y_3 = y_5 = \eta$; $y_2 = y_4 = y_K = \xi$:

$$\mathbf{\Lambda}^{2/K} = \Lambda_\eta(2h\xi)\Lambda_\xi(-2h\eta).$$

We can always choose ξ and η positive. Therefore we only have to maximize the eigenvalue (18) within the two-parameter space

$$\xi = \frac{2n - N}{N} \qquad \eta = \frac{2m - N}{N} \qquad n, m = 0, 1 \ldots \frac{N}{2}.$$

By means of the Newton–Ralphson method we are able to solve BA equations directly and find the block with the largest eigenvalue for system size up to $N = 32$.

It turns out, however, that the maximal eigenvalue for all values of parameters a, b, c and h belongs either to the block $n = m = N/2$ (in which case h vanishes from all equations (15), (16), yielding the known results for the six-vertex model), or to the block with at least one of n, m, say m equal to zero: $m = 0$. Finally the Bethe ansatz (15), (16) can be rewritten

$$\mathbf{\Lambda}^{2/K} = \Lambda_{m=0}(2h\xi)\Lambda_\xi(2h) = \Lambda_1\Lambda_2$$

$$\Lambda_1 = a^N \mathrm{e}^{2h(2n-N)} + b^N \mathrm{e}^{-2h(2n-N)}$$

$$\Lambda_2 = a^N \mathrm{e}^{2hN} \prod_{j=1}^{n} \frac{a\tau_j - b(2\Delta\tau_j - 1)}{a - b\tau_j} + b^N \mathrm{e}^{-2hN} \prod_{j=1}^{n} \frac{b - a(2\Delta - \tau_j)}{-a + b\tau_j}$$

$$\mathrm{e}^{4hN}(\tau_j)^N = (-1)^{n+1} \prod_{l=1}^{n} \frac{\tau_j\tau_l - 2\Delta\tau_j + 1}{\tau_j\tau_l - 2\Delta\tau_l + 1}.$$

Note that the eigenvalue is invariant under the transformation

$$a \to b \qquad b \to a \qquad h \to -h.$$

Figures 3(a)–(d) show the phase diagram of the model in the space of Boltzmann weights ratios a/c, b/c, for the different values of interplane constant h. Figure 3(a) (decoupled planes, $h = 0$) repeats well known results for usual six-vertex model: the three distinct phases exist separated by the lines $\Delta = \pm 1$. These phases are (for details see [8]):

(I) Antiferroelectric phase. C-vertices (types 5 and 6) are dominant; in sufficiently low temperatures vertex plane configuration is filled with arrows alternating in both directions with step 1.

(II) Disordered phase $-1 < \Delta < 1$. All types of vertices are present; there are no types of vertices which are dominant. Here lies the high-temperature limit, so one should expect disorder.

(III) Ferroelectric phase $\Delta > 1$. Phase III occupies two separated regions, the upper left and the bottom right in the phase diagram. In the upper left region, $b/c > a/c + 1$, each plane is occupied by either exclusively type 3, or exclusively type 4 vertices. It is convenient to consider the arrow resulting from vector summation of all arrows in the plane: for the type 3 configuration, all arrows on the plane are pointing up and to the left, resulting is up-left arrow $\nwarrow$, whereas for the type 4 configuration, the resulting is down-right arrow $\searrow$, see figure 2. Polarization vector (14) modulus reaches its maximum $|y| = 1$, namely, $y = 1$ for the type 3 configuration and $y = -1$ for the type 4 configuration.

If we associate with each plane k the corresponding arrow: $\nwarrow$ for type 3, $\searrow$ for type 4, then the state of the multiplane model in phase III, upper left region, is characterized by the random sequence

$$\ldots \nwarrow \searrow \searrow \nwarrow \searrow \nwarrow \nwarrow \nwarrow \ldots \tag{38}$$

consisting of these arrows randomly placed. Of course switching on some vanishing external field favouring type 3 configuration will lift up this degeneracy, giving the homogeneous sequence

$$\ldots \nwarrow \nwarrow \nwarrow \nwarrow \nwarrow \nwarrow \nwarrow \ldots .$$

The state of the model in the bottom right region, phase III, $a/c > b/c + 1$ will be analogously characterized by the type 1, type 2 vertices configurations, or up-right, down-left $\nearrow$, $\swarrow$ arrows:

$$\ldots \nearrow \nearrow \nearrow \swarrow \nearrow \swarrow \swarrow \nearrow \ldots .$$

In figures 3(*b*)–(*d*) the phase diagrams for the systems with a fixed h in increasing order are given. The phases I–III are exactly the same as in the uncoupled planes limit in figure 3(*a*). For nonzero coupling h the regions occupied by phase III are given by the formula $\Delta = \cosh 4h$, and two new phases arise.

(IV) Layered antiferroelectric phase. This phase is exactly the one described as the strong interplane coupling limit in section 2. Each plane is in the ferroelectric phase, but plane $k + 1$ configuration strictly follows from one in the kth plane by $\pi/2$ clockwise rotation. So, the plane-layers in increasing order are formed by the unique, up to shifting, sequence of vertices, or the resulting arrows:

$$\ldots \nearrow \searrow \swarrow \nwarrow \nearrow \searrow \swarrow \nwarrow \ldots$$

(compare with the sequence (38)).

In that phase polarization vectors (14) alternate every other plane $y_{k+2} = -y_k$:

$$\ldots y_k, y_{k+1}, \ldots = \ldots 1; -1; -1; 1; 1; -1; -1; 1 \ldots \tag{39}$$

forming the layered antiferroelectric structure (in each separate plane the structure is ferroelectric). Polarization vector modulus in each plane reaches its maximal value $|y_k| = 1$, any k.

(V) Phase V is an intermediate phase which can be described as follows. The system splits into two subsystems, each contains two planes, kth and $(k + 2)$th, e.g. 'the first and the third' and 'the second and the fourth'. In one of the subsystems the planes are

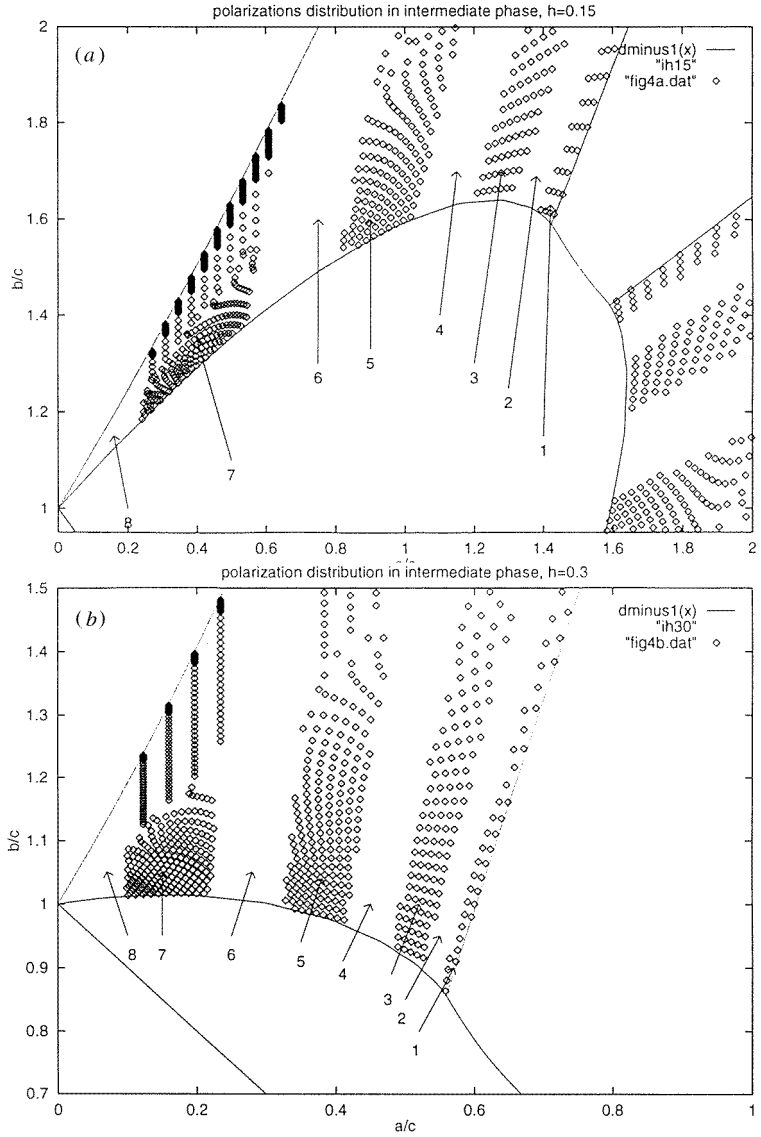

Figure 4. Distribution of polarizations in the intermediate phase V. This phase is characterized by the periodically repeated set of polarizations (in planes) (36) $\{1\ -\xi\ -1\ \xi\ \ldots\}$, $\xi = (2n-N)/N$, n being the number of upward pointing arrows in a row in the corresponding plane. The results of numerical calculations of ξ for the system size $N = 32$ are shown. The area is divided into eight sectors, sector number k corresponds to $2k-1 \leqslant n \leqslant 2k$. Thus, polarization monotonically increases from $\xi = -1$ on the second-order phase transition line to $\xi = 0$ near the point $(0, 1)$. On the 'free-fermions' circle $\Delta = 0$ inside the intermediate phase, the exact value of ξ is given by $\sin(\pi\xi/2) = -(a/b)\sinh(4h)$.

in ferroelectric phase, with alternating polarization vector $y_k = 1$, $y_{k+2} = -1$. Another subsystem is partially disordered: $y_{k+1} = 2x - 1 = -y_{k+3}$. Again, as the previous one, this structure has period 4. Within the phase 4, x varies (see figures 4(a) and (b)); on the transition line between phases IV and V, x goes to zero continuously, forming the strong

interplane coupling structure in phase 4. For the free-fermions limit, $\Delta = 0$, or $a^2+b^2 = c^2$, the value of x is known exactly (see [5]):

$$\cos \pi x = \frac{a}{b} \sinh 4h \qquad \text{for } a < b. \tag{40}$$

Outside the free-fermions curve, the branches with equal polarizations are arranged quite regularly, as is seen from figures 4(a) and (b). However, we cannot present the exact formula for the moment.

The analytical and numerical calculations show that there are no other phases in the phase diagram.

The second-order phase transition between the phases V and IV can be found considering the equality

$$\mathbf{\Lambda}(n/N \to 0) = 1. \tag{41}$$

Proceeding analogously to [8] we get

$$\tau_j = \mathrm{e}^{-4h}.$$

For $a\mathrm{e}^{4h} > b$, $b > a$ we have

$$\prod \frac{a\tau_j - b(2\Delta\tau_j - 1)}{a - b\tau_j}\mathrm{e}^{-4h} = \prod \frac{a - 2b\Delta + b\mathrm{e}^{4h}}{a\mathrm{e}^{4h} - b}\mathrm{e}^{-4h} = 1$$

and $\frac{a}{b} \sinh 4h = 1 - \Delta\mathrm{e}^{-4h}$, or using (17),

$$b/c = (a/c) \exp(4h) - 1. \tag{42}$$

All phase curves are symmetrical with respect to $a = b$ line.

Proceeding with the same equality (41) and taking $b > a\mathrm{e}^{4h}$, we obtain

$$\Delta = \cosh 4h. \tag{43}$$

But now this line marks only the right margin for the phase transition III/V, and not necessarily the exact point. We have found, however, with all numerical accuracy, that line (43) is indeed the exact transition point. With increasing h, the phases IV and V expand in space, and the others diminish. When h reaches $h_1 = 0.458\,134\ldots$ and higher, phase II disappears completely as is shown in figure 3(d). The fraction of space occupying by the phases II, III diminishes exponentially with h, as is seen from (42), (43).

Finally, the transition line between the phases II/IV (II/V) or I/IV (I/V) in figures 3(b)–(d) is obtained numerically. The line ends in points $(0, 1)$ and $(1, 0)$ which agrees with the limiting 'Ising chain' case. Phase transition II/IV (II/V) or I/IV (I/V) is of the first order. Indeed in phases II or I the partition sum does not depend on h at all (all $n_k \equiv N/2$ and polarization vector y_k for all k is zero). The values of the y_k-set jump when crossing the critical curve and the dependence on h show up. So the partition sum will have a cusp as a function of h.

The transition IV/V is of the second order. On this line, the order parameters—polarization vectors y_k (equation (14)) change continuously when approaching the critical point. The second derivative for free energy over h diverges as the inverse square root $\sim 1/\sqrt{h - h^*}$ in the critical point (Pokrovsky–Talapov-type transition [9]).

We have described the phase diagram of the 3D-extended model with the homogeneous set of constants. The phase diagrams for the models with arbitrary sets of 'h' and '$-h$' constants are the same, with redefinition of phases (see equations (22)–(24)). Note that for the model with alternating constants, $\{\ldots h, -h, h, -h, \ldots\}$, the period is always 2 (in planes).

9. Conclusion

We have obtained the phase diagram for the 3D solvable multilayered six-vertex model, in full three-parameter space. The model enjoys locality of interactions and positivity of Boltzmann weights. The applicability of the method to other solvable vertex models with the ice rule (46) is shown in [6]. In view of possible applications, note that the strength of layer–layer interaction h can vary from plane to plane, as well as the anisotropy parameter within each layer. Another possibility is to include more distant than nearest-neighbour interactions along third axis. The resulting solvable models are ones with competing interactions [7].

Another interesting question is the universality class of the model we have considered. The finite size scaling analysis (see e.g. [10]) of new (due to plane–plane coupling) critical phase, named V in the phase diagram, shows that it is described by a 2D conformal field theory with central charge $c = 1$. Thus it belongs to the same universality class as the 'source' six-vertex model.

Acknowledgments

One of the authors (VP) thanks colleagues from the Institute for Theoretical Physics, University of Amsterdam, where this work was mainly done, for the hospitality, and Professor Doochul Kim for a nice introduction to finite size scaling. This work was supported in part by the INTAS grants 93-1324, 93-0633, Soros grant K5Z100 and by the Erwin Shrödinger Institute, Vienna. This work was supported in part by the Korea Science and Engineering Foundation through the SRC program. We thank referees for good comments.

Appendix

The partition function for the system with open boundaries is given by

$$\mathbf{Z} = \mathcal{T}^M$$

where $\mathcal{T}$ is the global monodromy matrix. In our case (see equations (3)–(11)) $\mathcal{T}$ factorizes into the product

$$\mathcal{T} = \prod_{k=1}^{K} \mathcal{T}_k \tag{44}$$

where the 'local monodromy matrix' for the kth plane

$$\mathcal{T}_k = \prod_{n=1}^{N} \mathrm{e}^{-h_k \sigma^{(k)} \tau_n^{(k+1)}} L_n^{(k)} \mathrm{e}^{h_{k-1} \sigma^{(k)} \tau_n^{(k-1)}}$$

L_n being the matrix of Boltzmann weights for the six-vertex model; upper index (k) corresponds to the kth plane, and matrices σ and τ are defined by (12). Omitting the index k in the right-hand side of the last formula for convenience and denoting

$$\sigma^{(k)} \to \sigma \qquad \tau_n^{(k+1)},\ \tau_n^{(k-1)} \to \tau_n',\ \tau_n'',\ h_k \to h,\ h_{k-1} \to g$$

we have

$$\begin{aligned} \mathcal{T}_k(h, g) &= \prod_{n=1}^{N} \mathrm{e}^{-h\sigma\tau_n'} L_n \mathrm{e}^{g\sigma\tau_n''} \\ &= \mathrm{e}^{-h\sigma\tau_1'} L_1 \mathrm{e}^{g\sigma\tau_1''}\ \mathrm{e}^{-h\sigma\tau_2'} L_2 \mathrm{e}^{g\sigma\tau_2''} \ldots \mathrm{e}^{-h\sigma\tau_N'} L_N \mathrm{e}^{g\sigma\tau_N''}. \end{aligned} \tag{45}$$

The exponential factors in this expression commute with each other because they are diagonal matrices (see (12)). The commutation with L_n is given by

$$[\exp(h(\sigma+\tau_n)\tau_p''), L_n] = [\exp(h(\sigma+\tau_n)\tau_p'), L_n] = 0$$

which is equivalent [5, 6] to the charge conservation property of the 'source' six-vertex model (4):

$$L_{6v\,\alpha'\beta'}^{\alpha\beta} = 0 \qquad \text{unless } \alpha'+\beta' = \alpha+\beta. \tag{46}$$

Using these commutation rules, we move all exponents in (45) outside to the left and to the right. For instance, to move the term $\mathrm{e}^{-h\sigma\tau_2'}$ to the left, one inputs the unity

$$\mathrm{e}^{-h\sigma\tau_2'}\mathrm{e}^{\pm h\tau_1\tau_2'} = \mathrm{e}^{-h(\sigma+\tau_1)\tau_2'}\mathrm{e}^{h\tau_1\tau_2'}.$$

The first factor in this expression commutes with L_1 and goes to the left while the second one commutes with all $L_1, L_2, \ldots L_N$ (because they act in the different subspaces) and goes to the right. Repeating the similar procedure for all exponents, and taking into account $\sum_{m=2}^{N}\sum_{n=1}^{m-1} = \sum_{n=1}^{N-1}\sum_{m=n+1}^{N}$, we obtain

$$\begin{aligned} &\mathcal{T}_k(h,g) = A_k \mathrm{e}^{-h\sigma\sum_{n=1}^{N}\tau_n'}\mathcal{T}_k(0,0)\mathrm{e}^{g\sigma\sum_{n=1}^{N}\tau_n''}A_k^{-1} \\ &A_k = \exp\left\{\sum_{m=2}^{N}\sum_{n=1}^{m-1}(-h\tau_m'\tau_n - g\tau_m\tau_n'')\right\}. \end{aligned} \tag{47}$$

Then, due to the charge conservation (46), $\sum_{n=1}^{N}\tau_n^{(k)}$ is a constant. For the six-vertex model this property is known also as the ice rule (see e.g. [1, 8]):

$$\frac{1}{N}\sum_{n=1}^{N}\tau_n^{(k)} = y_k$$

—the so-called polarization vector. y_k may take values $-1 \leqslant y_k \leqslant 1$.

Restoring the index k, A_k can be written as

$$A_k = C_{k+1,k}C_{k,k-1} \qquad C_{k+1,k} = \exp\left\{\sum_{m=2}^{N}\sum_{n=1}^{m-1}(-h_k\tau_m^{(k+1)}\tau_n^{(k)})\right\}.$$

Multiplying $\mathcal{T}_1\mathcal{T}_2\ldots\mathcal{T}_K$ and using $A_k^{-1}A_{k+1} = C_{k,k-1}^{-1}C_{k+2,k+1}$, we get for the global monodromy matrix (9):

$$\begin{aligned} \mathcal{T} = {} & C_{1,0}C_{2,1}\mathrm{e}^{-h_1\sigma^{(1)}Y_2}\mathcal{T}_1(0,0)\mathrm{e}^{h_0\sigma^{(1)}Y_0}C_{1,0}^{-1}C_{3,2} \\ & \ldots C_{K-1,K-2}^{-1}C_{K+1,K}\mathrm{e}^{-h_K\sigma^{(K)}Y_{K+1}}\mathcal{T}_K(0,0)\mathrm{e}^{h_{K-1}\sigma^{(K)}Y_{K-1}}C_{K+1,K}^{-1}\ C_{K,K-1}^{-1}. \end{aligned}$$

Here $Y_k = Ny_k$.

Moving C-factors (C^{-1}-factors) to the left (to the right), one obtains

$$\begin{aligned} &\mathcal{T} = B\left(\prod_{k=1}^{K}\mathrm{e}^{-h_k\sigma^{(k)}Y_{k+1}}\mathcal{T}_k(0,0)\mathrm{e}^{h_{k-1}\sigma^{(k)}Y_{k-1}}\right)B^{-1} \\ &B = \prod_{k=1}^{K}C_{k,k-1}. \end{aligned} \tag{48}$$

B depends only on $\tau_n^{(k)}$, and therefore it is a gauge transformation. In the other hand, one can consider the transfer-matrix for the six-vertex model in a horizontal field of strength H:

$$\mathcal{T}_{6v}(H) = \prod_{n=1}^{N}\mathrm{e}^{-\frac{H}{2}\sigma}L_n\mathrm{e}^{-\frac{H}{2}\sigma}.$$

Using the same procedure, we arrive at formula (47) with substitution $h = -g = H/2$; $\tau_n', \tau_n'' \to 1$:

$$\mathcal{T}_{6v}(H) = A\mathrm{e}^{-\frac{NH}{2}\sigma}\mathcal{T}_{6v}(0)\mathrm{e}^{-\frac{NH}{2}\sigma}A^{-1}$$

in which A again is a gauge transformation. Comparing the last relation with (48), we see that partition function of our model and the set six-vertex planes, kth plane in a field

$$H_k = h_k y_{k+1} - h_{k-1} y_{k-1}$$

(both systems with open boundaries) are gauge-equivalent. Hence, their transfer-matrices are equal:

$$\mathbf{T}_{our\ model} = \prod_{k=1}^{K} T_{6v}(h_k y_{k+1} - h_{k-1} y_{k-1}).$$

References

[1] Baxter R J 1982 *Exactly Solvable Models in Statistical Mechanics* (London: Academic)
[2] Zamolodchikov A B 1980 *Sov. Phys.–JETP* **52** 325; 1981 *Commun. Math, Phys.* **79** 489
[3] Bazhanov V V and Baxter R J 1992 *J. Stat. Phys.* **69** 453
Mangazeev V V, Sergeev S M and Stroganov Yu G 1994 New series of 3D lattice integrable models *Int. J. Mod. Phys.* A **9** 5517
[4] Takhtajan L A and Faddeev L D 1979 *Usp. Mat. Nauk.* **34** 13 (Engl. transl. 1979 *Russ. Math. Surv.* **34** 11
[5] Borovick A E, Kulinich S I, Popkov V Yu and Stzhemechny Yu M 1996 *Int. J. Mod. Phys.* B **10** 443–53
[6] Popkov V Yu 1994 Anisotropic extension of 2D solvable models of statistics to 3D *Phys. Lett.* A **192** 337
[7] Popkov V, Enolskii V and Salerno M 1996 Exactly solvable multilayered 3D statistical model with competing interactions: connections with ANNNI model *Preprint* SNUTP 96-020
[8] Lieb E H and Wu F Y 1972 *Phase Transitions and Critical Phenomena* vol 1, ed C Domb and M Green (New York: Academic) p 436
[9] Pokrovsky V L and Talapov A L 1980 *Sov. Phys.–JETP* **51** 134
[10] Noh J D and Kim D 1996 *Phys. Rev.* E **53** 3225